Food Chemistry: X 23 (2024) 101537

Contents lists available at ScienceDirect

Food Chemistry: X

journal homepage: www.sciencedirect.com/journal/food-chemistry-x

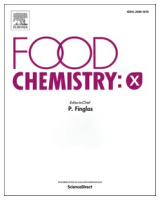

The physicochemical properties of Cassava Starch/Carboxymethyl cellulose sodium edible film incorporated of *Bacillus* and its application in salmon fillet packaging

Xiqian Tan [*], Anqi Sun [1], Fangchao Cui, Qiuying Li, Dangfeng Wang, Xuepeng Li, Jianrong Li [*]

College of Food Science and Technology, Bohai University, Jinzhou, Liaoning 121013, China

ARTICLE INFO

Keywords:
Film properties
Food packaging
Bacillus
Antioxidant
Antibacterial
Polymer

ABSTRACT

Edible film is now a trend in the food packaging industry. In this study, edible films were prepared by adding two *Bacillus* spp. (*Bacillus amyloliquefaciens* Y11 and *Bacillus velezensis* Y12) to a cassava starch and carboxymethyl cellulose sodium matrix. The structural, physicochemical, and biological characteristics of the film were analyzed, and its application in salmon preservation was explored. The film had a dense structure and no pores, indicating that its polymeric components were compatible with each other. The addition of *Bacillus* spp. increased the antioxidant activity of the film and its ability to eliminate hydroxyl radicals (84.57% and 91.86%, respectively). The film also showed good antibacterial activity against several pathogens and underwent complete degradation in natural soil within 12 days. The film significantly reduced the total coliform count of salmon and extended its shelf life by 3 days, demonstrating its value as a food-packaging material.

1. Introduction

Food packaging often relies on synthetic plastics for their superior waterproof properties, flexibility, and cost-effectiveness characteristics. However, the poor biodegradability of synthetic polymers causes environmental pollution. Consequently, to address plastic pollution, a shift towards active, highly renewable, and degradable packaging has emerged in the food packaging industry. Edible films are packaging materials made from safe-to-consume substances and demonstrate better solubility and biodegradability than conventional plastic films, serving as an eco-friendly solution to the plastic pollution problem (Dehghani, Hosseini, & Regenstein, 2018) and at the meantime could offer structural stability and can protect foods from contaminants and pathogens (Abdollahzadeh, Nematollahi, & Hosseini, 2021).

Polysaccharides are favored as natural matrices for edible films due to their hydrophilicity, selective permeability to CO_2 and O_2, and ability to prevent lipid migration. Currently, the commonly used polysaccharide matrices include cellulose, starch, pectin derivatives, and seaweed extract (Dehghani et al., 2018). Among these, cassava starch (CS) is favored for its superior film-forming properties, which result from its high amylose content (17%), and advantages such as low pasting temperature, excellent gel stability, and transparency (Bangyekan, Aht-Ong, & Srikulkit, 2006). However, films made solely from CS often exhibit poor tensile properties due to its hydrophilicity. Hence, CS is frequently blended with other natural polymers and plasticizers. Carboxymethyl cellulose sodium (CMC), known for its non-toxicity, ease of film formation, toughness, and biodegradability, serves as an excellent complement to CS in producing edible films (Ghanbarzadeh, Almasi, & Entezami, 2010). Glycerol is also preferred as a plasticizer for its stability and compatibility with hydrophilic biopolymers (Jaderi, Yazdi, Mortazavi, & Koocheki, 2023).

Additionally, the edible film matrix could serve as a carrier for natural antioxidants and antibacterial agents, enhancing their food preservation abilities (Gürdal & Çetinkaya, 2023). Common additives in edible films include plant extracts (e.g., thyme, grape seed, and green tea extract), organic acids (e.g., benzoic acid and sorbate), enzymes (e.g., lysozyme), bacteriocins (e.g., lactostreptococcin), metal nanoparticles (e.g., gold, silver, and zinc), and probiotics. These additives reinforce the technical and functional properties of edible biofilms (Xie et al., 2023). Films based on CS and CMC could also serve as effective carriers. Their antioxidant and antimicrobial properties were enhanced by adding functional substances like essential oils, polyphenols, and nanoparticles. For instance, edible films composed of CS/CMC incorporated with apple polyphenols (AP) have been found to significantly inhibit lipid oxidation

* Corresponding authors.
E-mail addresses: tanxiqian@163.com (X. Tan), lijr6491@163.com (J. Li).
[1] Co-first author.

https://doi.org/10.1016/j.fochx.2024.101537
Received 10 May 2024; Received in revised form 3 June 2024; Accepted 3 June 2024
Available online 4 June 2024

in chicken meat (Lin, Peng, Chen, Li, & Cui, 2023). Similarly, films containing caffeic acid-loaded silica nanoparticles within a CS/CMC matrix can display strong antioxidant and antimicrobial efficacy, effectively inhibiting *Escherichia coli* and *Staphylococcus aureus* growth in meat while also delaying lipid oxidation and pH elevations (Lin et al., 2023).

Among the candidates for the additives of the edible films, probiotics have recently gained great traction, and research has shown promising results (Saleena, Kumaran, How, & Pui, 2023). In one study, extracellular polysaccharides (EPS)-producing *Lactobacilli* were incorporated into an edible cassava starch (CS) and carboxymethyl cellulose sodium (CMC) substrate. This study proved that probiotics could be evenly dispersed within the edible film, enhancing its antioxidant capability while effectively providing protection from water and UV rays. Thus, this edible film was suitable for banana packaging (Lin et al., 2020). Further, Ceylan and Atasoy (2023) demonstrated that *Lactobacillus rhamnosus* GG integrated oligofructose and inulin on sodium caseinate films could significantly reduce water loss and prevent undesirable changes in acidity and hardness in cheese slices than the film without the probiotic. Moreover, Davachi, Pottackal, Torabi, and Abbaspourrad (2021) incorporated probiotics into seed mucus films derived from papaya, flax, and basil, confirming their preservatory effects on fruits and vegetables.

Bacillus species find extensive applications in food preservation and biocontrol owing to their unique ability to produce endophytic spores resistant to heat, UV radiation, and desiccation. Additionally, they secrete secondary metabolites like lipopeptides, polypeptides, and polysaccharides, which are biodegradable, non-toxic, highly stable, and possess bacteriostatic properties. Especially certain EPS produced by some *Bacillus* species has remarkable physicochemical properties and characteristics, including emulsification, heavy metal sequestration, bioflocculation, antibacterial, antibiofilm, and antioxidant. A certain amount of *Bacillus* strains could serve as potential probiotics due to their remarkable functions (Chowdhury, Hartmann, Gao, & Borriss, 2015). However, the investigation of the probiotic *Bacillus*-embedded edible film needs to be further explored. Moreover, many edible films currently focus on preserving fruit and vegetables; their application on preserving salmon, a very popular ready-to-eat seafood, would be worth studying.

In a previous study, two *Bacillus* strains — *Bacillus amyloliquefaciens* Y11 and *Bacillus velezensis* Y12 — were isolated from shrimp paste and were found to possess exopolysaccharides-producing, antimicrobial, antioxidant, and biofilm-inhibition properties (Tan, Wang, Cheng, Li, & Li, 2023). However, the impact of incorporating these strains into CS/CMC-based edible films on the films' physicochemical properties, bioactivity, and preservation efficacy remains unclear. Therefore, this study developed edible films incorporating *B. amyloliquefaciens* Y11 (Y11) and *B. velezensis* Y12 (Y12) into CS/CMC substrates. The objective was to assess the physicochemical properties and bioactivity of the resulting film and its preservation effects on salmon fillets.

2. Material and methods

2.1. Materials

CS was purchased from Wanyubang Ltd. (Henan, China); CMC (viscosity: 800–1200 mPa), glycerin, Ascorbic acid (Vc), 2,2′-Azinobis-(3-ethylbenzthiazoline-6-sulphonate) (ABTS) and potassium persulfate was purchased from Aladdin (Shanghai, China); 1-diphenyl-2-picrylhydrazyl (DPPH) was purchased from Yuanye Bio-technology Ltd. (Shanghai, China). All other reagents were of analytical grade. Luria-Bertani (LB) broth was purchased from Aoboxing Biology Technology (Beijing, China). Y11 and Y12, which had antibacterial and EPS-producing abilities, were previously isolated from shrimp paste (Tan et al., 2023) and preserved in the China General Microbiological Culture Collection Center (CGMCC; CGMCC No. 27124 and CGMCC No. 27125, respectively).

2.2. Preparation of the Bacillus power

Y11 and Y12 were inoculated in LB liquid medium (2% inoculum) and placed in a 37 °C shaker. After incubation (24 h), the cultures were centrifuged (5180 × *g*, 10 min, 4 °C). The pellets were rinsed with sterile water and centrifuged again for 10 min. The above steps were repeated twice. The bacterial powder was prepared using 1% maltodextrin, 4.74% alginate, and 1.45% glycerol. A protective agent was added to the suspension of bacteria in sterile water (mass ratio of bacteria to protective agent = 1:2). The suspension was poured into Petri dishes and placed at −80 °C for pre-freezing before freeze-drying to obtain the bacterial powder.

2.3. Preparation of the edible film

Briefly, 4 g CS and 1.5 g glycerol were added to 100 mL of distilled water and heated at 80 °C with stirring until the starch was entirely gelatinized. Then, 0.2 g CMC was added and the solution was heated at 80 °C to ensure CMC was completely dissolved. After cooling, 0.3 g Y11 and Y12 powders were added to the above mixture separately to prepare the CS/CMC/Y11 and CS/CMC/Y12 film solutions. The film solution containing no bacteria was named CS/CMC. Subsequently, the film solutions were allowed to settle in a water bath for 30 min to remove any foam. Finally, different film solutions were poured into the disposable Petri dish (diameter, 90 mm) and dried in a blast drying oven (DHG-9055 A, Shanghai Yiheng Technology Instrument Co., Ltd., Shanghai, China) at 30 °C (Fig. 1).

2.4. Viability of the Bacillus strains

The viability of Y11 and Y12 in the films was investigated before and after drying and every 5 d during the 30-day storage period using the plate count method (Lacey, López-Caballero, Gómez-Estaca, Gómez-Guillén, & Montero, 2012). Briefly, 1 g of film liquid or film was blended with 9 mL of sterile phosphate-buffered saline (PBS) and incubator at 37 °C for 24 h. Then, the bacterial suspensions were serially diluted 10-fold (1 mL bacterial suspension + 9 mL sterile water) , spread on LB medium, and incubated for counting the bacterial colonies.

2.5. Rheological properties of the film solution

The rheological properties of the film solutions were determined using a rheometer (HAAK, Thermo Fisher Scientific, USA) equipped with a core and plane geometry system (50-mm diameter, 1-mm gap). The steady flow behavior was measured under a 0.1–100 s^{-1} shear rate range at 25 °C.

2.6. Scanning electron microscopy (SEM)

The microstructure of the film surface was evaluated using SEM with a cold-field-emission scanning electron microscope (ZEISS, Sigma500, Japan) at an accelerating voltage of 5.0 kV.

2.7. Evaluation of physical properties

2.7.1. Thickness and density

The films prepared using the petri dishes were used to test the thickness and density of the film. Four randomly selected points on the film (excluding the center) were evaluated using a micrometer. Film thickness (h) was expressed as the average of the readings obtained (mm).

The density ρ (g/cm^3) of the film was expressed as described in Eq. (1), where m (g) was the mass of the film (diameter, 90 mm) measured by the electronic scale and s (m^2) was the surface area of the 90 mm petri dish (average 63.585 cm^2).

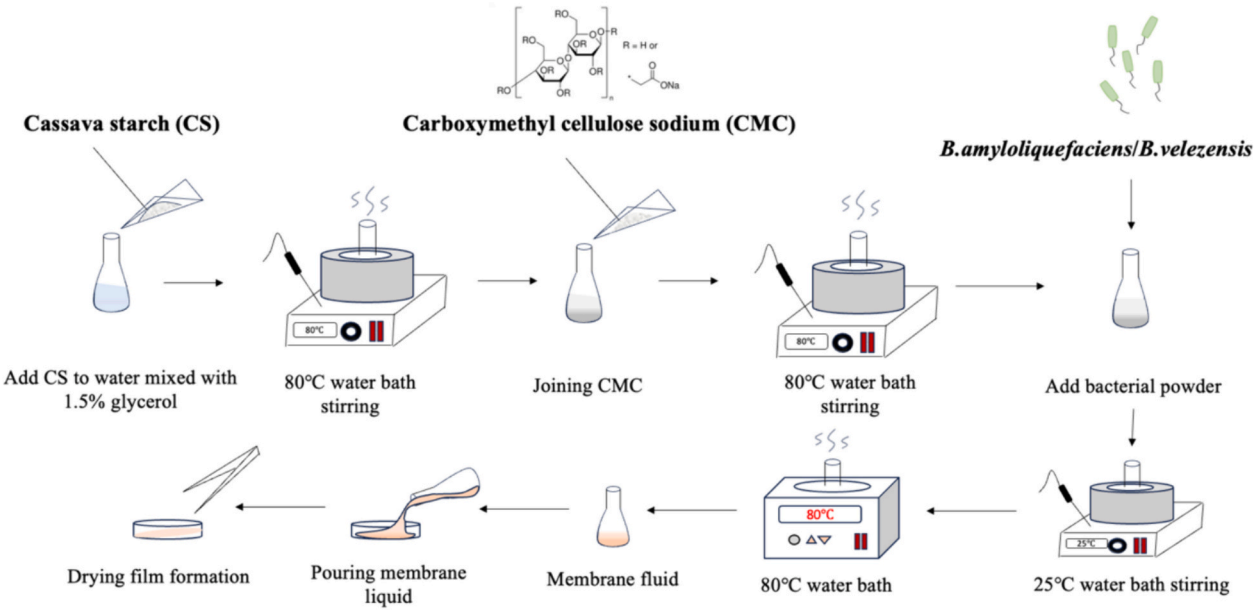

Fig. 1. Schematic diagram of film preparation.

$$\rho\ (g/cm3) = \frac{m}{s \times h} \quad (1)$$

2.7.2. Moisture content (MC) and swelling rate (SW)

The MC of the film (20 × 20 mm) was dried in the oven to a constant weight at 105 °C, and the final weight was recorded as M_1. Moisture content was calculated using Eq. (2), where M_0 represented the initial weight.

$$\text{Moisture content}\ (\%) = \frac{M0 - M1}{M0} \times 100 \quad (2)$$

The films were dried to constant weight (initial weight, W_0) at 105 °C, then placed in 5 mL distilled water, after 12 h, its weight which the excess water was removing using a filter paper was recorded 12 h (W_1). The SW of the film was calculated using Eq. (3).

$$\text{Swelling rate}\ (\%) = \frac{W1 - W0}{W0} \times 100 \quad (3)$$

2.7.3. Contact angle

The contact angle of the rectangular film sheet (2 × 1 cm) was measured using a video optical contact angle meter (OCA25, Data Physics Instruments, Germany).

2.7.4. Water vapor permeability (WVP)

WVP represents the amount of water vapor that can be transmitted through a film sized 1 m^2 at a certain temperature, relative humidity, and water vapor pressure difference within 24 h. We used the water vapor permeability test method cup method (GB 1037–1988) as the standard and modified it as described by Nazir and Wani (2022). The film was cut into round pieces (diameter, 45 mm), and the film samples were fixed on a cylindrical test cup containing 50 mL distillate, with a 2 cm distance towards the water surface. The test cup was placed in a desiccator for 7 d at 25 °C, and its weight was recorded every 24 h. A time-dependent weight curve was plotted, and its slope was calculated to detect the water vapor transmission rate (WVTR). WVP was calculated according to Eq. (4) (L, thickness of the film; A, the effective area of the film [m^2]; and ΔP, difference in water vapor pressure between the two sides of the film [kPa]).

$$WVP = \frac{WVTR \times L}{\Delta P \times A} \quad (4)$$

2.7.5. Changes in color and brightness

The total color difference value (ΔE) indicates the change in the color of the composite film, and the whiteness index (WI) characterizes the degree of color on the surface of the composite film. ΔE was calculated by Eqs. (5), and WI was calculated by Eq. (6) (Gholam-Zhiyan, Amiri, Rezazadeh-Bari, & Pirsa, 2021), where L, a, and b represents the Hunter parameters of lightness, red-green, and yellow-blue, respectively. Notable, 5–6 replicate measurements were performed for each film using a colorimeter (CR-400, Konica Minolta, Japan).

$$\Delta E = \sqrt{(\Delta L^*)^2 + (\Delta a^*)^2 + (\Delta b^*)^2} \quad (5)$$

$$WI = 100 - \sqrt{(100 - L)2 + (a1)^2 + (b1)^2} \quad (6)$$

2.7.6. Opacity

The film was cut into several similar rectangle pieces as the optical side of a cuvette, and it was tightly affixed to the optical side of the cuvette. $OD_{600\ nm}$ was determined (A_{600}) (UV-2550, Shimadzu, Japan), and the opacity was calculated using Eq. (7); h was the thickness of the film (mm).

$$\text{Opacity} = \frac{A\ 600}{h} \quad (7)$$

2.8. Mechanical properties

The tensile strength (TS) of the film — defined as the maximum tensile stress that the sample could withstand under a tensile force until the point of rupture — was determined using a texture analyzer (TA-XTplus, SMS, Germany) (Razmjoo et al., 2021). The TS was calculated using Eq. (8) (F, tensile force sustained at break; L, thickness of the film [mm]; and W, width of the film [mm]).

$$TS\ (MPa) = \frac{F}{L \times W} \quad (8)$$

The maximum elongation at break (EBA) refers to the maximum deformation the film can withstand before it breaks. EBA was calculated using Eq. (9) (L, length of the elongated film at the point of breakage [mm] and L_0, original length of the film [mm]).

$$EBA(\%) = \frac{(L - L0)}{L0} \quad (9)$$

2.9. Differential scanning calorimetry (DSC)

DSC was measured using a differential scanning calorimeter (Q2000, TA Instruments, USA) (Mantovan, Bersaneti, Faria-Tischer, Celligoi, & Mali, 2018). Briefly, 3.0 mg film was placed in an aluminum crucible and heated at 10 °C/min from 50 °C to 350 °C.

2.10. Fourier transform infrared (FTIR) spectroscopy

FTIR spectroscopy (IRTracer, SHIMADZU, Japan) was performed in the spectral range of 4000–400 cm^{-1} under a spectral resolution of 4 cm^{-1} to evaluate the surface functional group of the film.

2.11. X-ray diffraction (XRD) analysis

The X-ray diffractometer (Ultima IV, Rigaku Corporation, Japan) was performed at a diffraction angle of 2θ from 0° to 100° at a speed of 5°/min to evaluate the crystallinity of the film.

2.12. Biodegradation rates

The biodegradability of the composite films was studied via soil degradation experiments (Sanhawong, Banhalee, Boonsang, & Kaewpirom, 2017). The film samples (2 × 2 cm) were buried in cups containing soil at a depth of about 8 cm from the surface. The soil temperature was about 25 °C, its relative humidity was 72%, its pH was 6, and its water content was 45%. After the samples were placed in the cups, the morphology of the films was observed and photographed daily.

2.13. Antioxidant activity

2.13.1. DPPH scavenging ability

The DPPH scavenging ability of the films was determined as described by Lin et al. (2020). Briefly, 200 μL of film solution was mixed with 200 μL 0.1 mM DPPH, and the absorbance value was measured at 517 nm before (A_{t0}) and 30 min after (A_{t30}) the reaction, and calculated using Eq. (10). Ascorbic acid (Vc) was used as a positive control.

$$\text{DPPH inhibition } (\%) = \frac{(At0 - At30)}{At0} \times 100 \quad (10)$$

2.13.2. $ABTS^+$ scavenging ability

For measuring $ABTS^+$ scavenging ability, 10 mg of ABTS was added to 2.6 mL of a 2.4 mmol/L potassium sulfate solution and incubated for 12–24 h in a light-proof environment to generate a stock solution of $ABTS^+$ radicals. Ethanol was used to adjust the concentration of the $ABTS^+$ solution such that its absorbance at 734 nm reached 0.70 ± 0.2. Then, 50 mg of the film sample was dissolved in 2 mL of methanol solution. After thoroughly mixing, the mixture was incubated for 3 h to obtain the sample solution. Subsequently, 2 mL of the $ABTS^+$ solution was added to the mixture and allowed to react for 30 min in the dark. After this, OD $_{734\ nm}$ of the mixture was measured. Distilled water and 1 mg/mL Vc solution were served as the negative and positive controls. $ABTS^+$ savaging ability was calculated using Eq. (11), where A_S and A_0 represent the OD $_{734\ nm}$ obtained after mixing the film or the distilled water with $ABTS^+$ solution, respectively.

$$\text{ABTS} + \text{scavaging rate } (\%) = \left(1 - \frac{AS}{A0}\right) \times 100 \quad (11)$$

2.13.3. Hydroxyl radical scavenging capacity

The hydroxyl radical scavenging capacity of the films was determined as described by Ye et al. (2019) and calculated using Eq. (12). The composition of the reaction systems included 1,10-phenanthroline (0.82 mL, 0.5 mM), ferrous sulfate (0.54 mL, 0.75 mM), and the film solution, all dissolved in phosphate buffer (1.09 mL, 0.2 M, pH 7.4). Subsequently, H_2O_2 (0.54 mL, 0.01%, *v*/v) was introduced and maintained at 37 °C for 1 h. The absorbance values of OD $_{536\ nm}$ before (A_0) and after (A_1) the reaction was measured. OD $_{536\ nm}$ of the uncompounded film was designated as A_S. Ascorbic acid (Vc) was used as the control.

$$\text{Hydroxyl radical scavenging capacity}(\%) = \frac{A1 - AS}{A0 - AS} \times 100 \quad (12)$$

2.14. Antimicrobial activity

The antibacterial properties of the films were assessed according to the method of Ma, Jiang, Ahmed, Qin, and Liu (2020). *Escherichia coli* and *Staphylococcus aureus* were used as the indicator strains. Pieces of the composite film were placed on a filter paper, which was then added to a Petri dish inoculated with *E. coli* or *S. aureus* and incubated at 37 °C for 24 h; the antibacterial properties of the films were estimated according to the size of the inhibition circle on the Petri dish.

2.15. Application of edible films in salmon preservation

2.15.1. Sample preparation

Fresh salmon fillets were cut into 2 × 2 cm pieces and weighed accurately. Control group fillets were left untreated. The experimental group fillets were wrapped in a CS/CMC, CS/CMC/Y11, or CS/CMC/Y12 film. All samples were refrigerated at 4 °C for 12 d. Samples were removed at 3-d intervals for evaluation.

2.15.2. pH

First, 1 g of the salmon was mixed with 9 mL of distilled water at a 1:9 ratio and homogenized for 3 min. Then, the pH of the supernatant was measured (PHS-25, INESA, ShangHai, China).

2.15.3. Total volatile basic nitrogen (TVB-N)

The TVB-N of salmon was determined according to a standard method (People's Republic of China GB 5009.228–2016: Determination of volatile basic nitrogen in food). First, 5 g of the salmon flesh was mixed with 40 mL of deionized water and homogenized. After 30 min of incubation, the filtered liquid was added to a distillation tube along with 0.5 g magnesium oxide and then distilled by a Kjeldahl nitrogen analyzer (Shandong Haineng Scientific Instrument Co., Ltd., DeZhou, ShanDong, China). Then 0.01 mol/L hydrochloric acid was used for calibration for the distillate. The concentration of hydrochloric acid was denoted as c, and the hydrochloric acid consumed during the calibration process was denoted as $\triangle V$ (mL); m represents the weight of the salmon samples; 14 (g/mol) was the mass of nitrogen equivalent to the standard titration solution a 1.0 mL of 0.01 mol/L hydrochloric acid. The content of volatile basic nitrogen (X) in the salmon was calculated as Eq. 13:

$$X(mg/100g) = \frac{\triangle V \times c \times 14}{m} \times 100 \quad (13)$$

2.15.4. Microbiological analysis

The microorganisms in the samples were analyzed using GB 4789.2–2022: Determination of total number of colonies in food microbiological examination (TVC), and GB 4789.3–2016: Food microbiological examination coliform count (TCB). First, 1 g of the sample was homogenized in 9 mL of normal saline for 5 min. The homogenate was serially diluted using normal saline. The dilutions were spread on agar and purple bile agar for microbiological analysis. After culture at 37 °C for 48 h, the number of colonies on the plate was counted to evaluate the TVC and TCB, respectively.

2.15.5. The color and texture profile analysis

The hardness, elasticity, cohesiveness, and chewiness of salmon pieces were determined through a texture analyzer (TA-XTplus, SMS, Germany) with a 1 mm/s measurement speed, a 2 s of recovery time, 50% of compression degree, 5 s of residence time, and 5 g of the trigger force. The probe type was p/50 (Li et al., 2022).

2.16. Statistical analysis

All parameters were examined in three parallel experiments. Data were analyzed by assuming a normal distribution and were subjected to analysis of variance (ANOVA). Means were compared using Tukey's test. All analyses were done using SPSS software. Results were considered significant at $p < 0.05$.

3. Results and discussion

3.1. Bacillus survival rate

The initial number of Y11 and Y12 was 15.13 ± 1.10 and 15.19 ± 1.01 log CFU/g, respectively. The viable bacterial count after freeze-drying was 10.46 ± 0.49 and 10.10 ± 0.09 log CFU/g, representing a survival rate of 69.13% and 66.49%. This indicated that the protective agent could greatly maintain the viability of Y11 and Y12.

3.2. Bacillus survival in films

3.2.1. Effect of drying

The drying process induces cellular osmotic and oxidative stress, resulting in the cytoplasmic membrane rupture due to water removal (Fu & Chen, 2011). This, in turn, affects bacterial activity. The survival of Y11 and Y12 is crucial for the beneficial antimicrobial effects of the composite biofilms and their in vivo probiotic effects after consumption. The survival of Y11 and Y12 in liquid and dried films is shown in Fig. 2a. The initial counts of Y11 and Y12 in the film solution were 6.64 ± 0.04 and 6.56 ± 0.10 log CFU/g, respectively. After the film was dried, the bacterial counts increased to 6.74 ± 0.06 and 7.03 ± 0.15 log CFU/g, respectively ($p < 0.05$). This suggested that Y11 and Y12 can survive in the CS/CMC matrix and that CS/CMC is suitable for the growth of these strains. Other research also proved that starch substrates can potentially protect probiotics (Espitia, Batista, Azeredo, & Otoni, 2016).

3.2.2. Time-dependent survival

To observe the survival of *Bacillus* in the CS/CMC matrix over time, samples were taken on the 5th, 10th, 15th, 20th, 25th, and 30th days after film formation. As shown in Fig. 2b, the number of *Bacillus* in both CS/CMC/Y11 and CS/CMC/Y12 remained within the range of 10^6–10^7 CFU·g^{-1} despite prolonged film storage. This indicated that both Y11 and Y12 maintained certain viabilities as the duration of storage increased. Majeed et al. (2016) found that *Bacillus coagulans* MTCC5856 also demonstrate good stability during food processing and storage. It might be due to the spore-forming ability of the *Bacillus*, which allows them to defend themselves against adverse environmental factors and nutrient deficiency, and the spores can germinate under appropriate conditions.

3.3. Rheology

The rheological properties of film-forming liquids affect the thickness, uniformity, and mechanical properties of the films. These properties also determine whether the edible films can directly be used to cover the surface of the food products. As shown in Fig. 2c, the film liquids of CS/CMC/Y11 and CS/CMC/Y12 were viscous under low shear stress, indicating that there were some interaction forces between CS/CMC, and Y11 and Y12, which made the liquid films viscous. With the increase in the shear rate, the viscosity of the system decreased gradually. Hence, the liquid films showed shear thinning.

3.4. Morphology

As shown in Fig. 2d, the surface of the CS/CMC film was relatively smooth and structurally dense, indicating that there was good interaction between starch and CMC. Additionally, there were a few irregular particles on the surface of the film, likely resulting from incomplete starch pasting (Lin et al., 2020) or uneven pouring of the film solution. The surface of the films containing the bacterial powder was rough and contained uneven particles. This was mainly due to the uneven mixing of the bacterial powder or the uneven pouring of the film solution. SEM can be used to evaluate the uniformity, layer structure, pores, cracks, surface smoothness, and thickness of biofilms. As shown in Fig. 2e, the surface of the Y12 composite film was denser and more convex than the surface of the Y11, which might indicate that Y11 had a better binding effect on CS and CMC than Y12.

3.5. Physical and functional properties

3.5.1. Density and WVP

The thickness of each film ranged from 0.02 mm to 0.045 mm, as shown in Table 1. The thickness of the films containing the bacterial powder tended to be lower than that of CS/CMC films. However, the difference was not significant because all the films were prepared with equal volumes of solutions, and the addition of bacterial powder had no significant effect on the thickness of the film. The density of the films was between 0.0035 and 0.0152 g/cm^2; the mean density of CS/CMC, CS/CMC/Y11, and CS/CMC/Y12 was 0.0039 ± 0.0001, 0.0040 ± 0.0004, and 0.0035 ± 0.0000 g/cm^2, respectively. Pereira et al. (2016) demonstrated that the addition of probiotics does not change the density of the films. However, our results showed the density of CS/CMC/Y11 was higher than that of CS/CMC/Y12, indicating that Y11 and the CS/CMC matrix show better interactions between each other and form more dense films. During the drying process, water evaporation would result in an increase in the thickness and density of the cassava matrix film. Furthermore, variations in molecular weight, interaction forces, and hydrogen bonds within the components of the film also affect their thickness and density.

WVP is an important parameter in food packaging materials. Lower WVP is associated with lower food dehydration rates and better food preservation. WVP is influenced by various elements, including the integrity of the film matrix, hydrophobicity, diffusion rate, solubility coefficient, the proportion of crystalline to amorphous regions, density, and polymer chain mobility. The WVP of the films is shown in Table 1. There were no significant differences between the three films. While other reports have indicated that the addition of probiotics could significantly reduce WVP, which might be due to the probiotics in the film matrix existing as discontinuous particles and effectively hindering polymer chain migration (Kanmani & Lim, 2013).

3.5.2. MC and SW

The MC of edible films affects the survival rate of probiotics within the film during storage, and lower water content would be more effective in preventing the deterioration of food (Lan et al., 2021). It was indicated (Table 1) that the addition of the bacteria did not change the MC of the film.

The SW of edible films determines their water resistance, which is an important parameter to consider while replacing traditional plastic packaging with edible films. The lower the SW, the higher the water resistance and the better the application prospect of the edible biofilm (Socaciu et al., 2020). The SW was not significantly different between CS/CMC and CS/CMC/Y11 (Table 1). However, the SW of CS/CMC/Y12 was significantly lower than that of CS/CMC ($p < 0.05$). These results indicated that the addition of Y12 to the CS/CMC matrix significantly improved ($p < 0.05$) the water resistance of the edible film. This may be

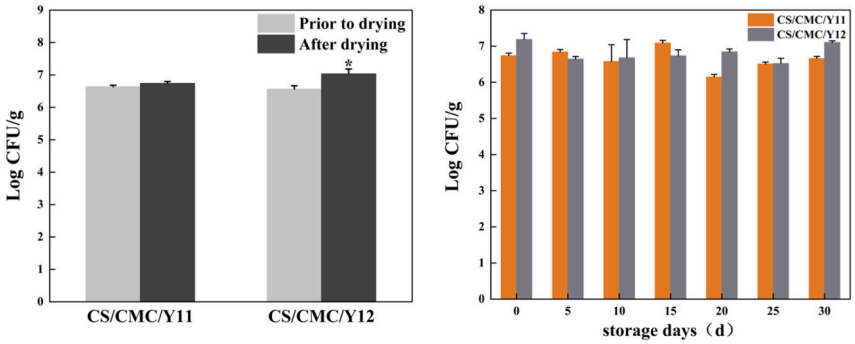

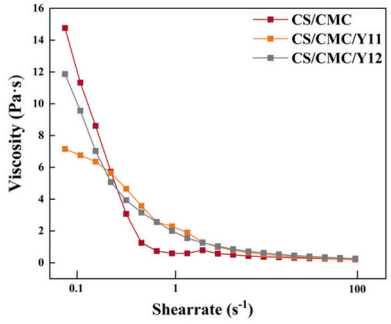

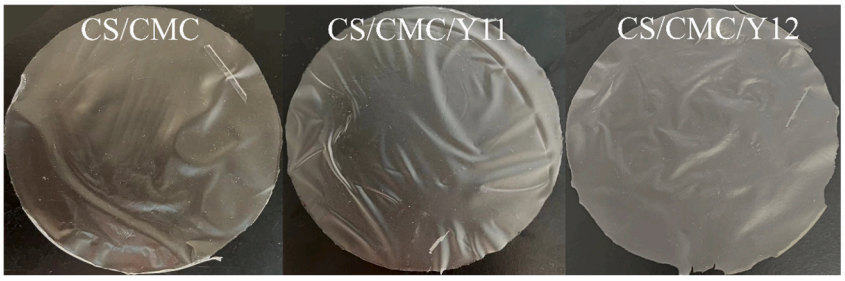

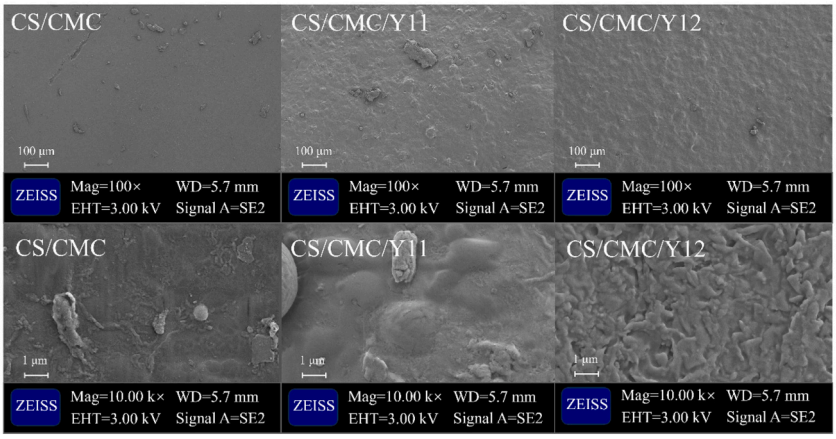

Fig. 2. Film-forming properties of the film. (a) The effect of drying on the *Bacillus* survival in the film; (b) Storage stability of Y11 and Y12 in the film; (c) Rheological properties of films; (d) Physical pictures of films; (e) SEM image of the films.

Table 1
Physiochemical characteristics of films.

Physiochemical characteristics	CS/CMC	CS/CMC/Y11	CS/CMC/Y12
Thickness (mm)	0.037 ± 0.015^{a}	0.032 ± 0.012^{a}	0.035 ± 0.006^{a}
Quality (g)	0.25 ± 0.01^{a}	0.25 ± 0.03^{a}	0.22 ± 0.00^{a}
Density(g/cm^2)	0.0039 ± 0.0001^{a}	0.0040 ± 0.0004^{a}	0.0035 ± 0.0000^{a}
WVTR(g/h)	0.031 ± 0.010^{a}	0.034 ± 0.016^{a}	0.029 ± 0.008^{a}
WVP × 10^6 (g/h·cm·Kpa)	2.17 ± 1.57^{a}	1.84 ± 0.85^{a}	1.71 ± 0.16^{a}
L	61.92 ± 0.56^{a}	61.37 ± 0.81^{a}	61.71 ± 1.19^{a}
a	-0.15 ± 0.01^{a}	-0.24 ± 0.06^{b}	-0.57 ± 0.08^{c}
b	0.22 ± 0.17^{c}	0.89 ± 0.27^{b}	2.29 ± 0.60^{a}
△E	20.43 ± 0.12^{a}	20.14 ± 0.31^{a}	19.17 ± 0.33^{b}
WI	61.92 ± 0.56^{a}	61.36 ± 0.81^{a}	61.60 ± 1.24^{a}
Opacity(A/mm)	10.65 ± 3.30^{b}	19.55 ± 2.20^{a}	9.90 ± 0.64^{bc}
Water contact angle (°)	93.17 ± 2.81^{b}	106.00 ± 1.03^{a}	94.42 ± 4.59^{b}
Moisture content (%)	24.42 ± 8.12^{a}	17.55 ± 2.58^{a}	26.43 ± 11.73^{a}
Swelling rate (%)	277.84 ± 7.95^{a}	275.20 ± 9.56^{a}	219.27 ± 49.73^{b}
TS (Mpa)	52.17 ± 5.68^{a}	52.17 ± 5.68^{a}	85.07 ± 33.80^{a}
EBA (%)	37.06 ± 13.32^{a}	22.76 ± 15.07^{ab}	12.83 ± 6.72^{b}

Notes: [a-c]Different letters in the same row indicate significant difference under the same condition ($p < 0.05$).

because CS/CMC/Y11 is not as dense as CS/CMC/Y12 and water molecules can pass through the pores in this film. Thus, the results showed that the water resistance of the CS/CMC film could be significantly improved by adding Y12 ($p < 0.05$). Moreover, no film breakage was detected during the experiment, demonstrating that all the films were stable.

3.5.3. Hydrophilicity

Food packaging materials, typically made of hydrophobic substances like plastic wrap, help prevent food spoilage. The hydrophilicity of an edible film can be determined based on its water contact angle (Al-Harrasi et al., 2022). The water contact angles of all films were >90° (Table 1), indicating that all the films were hydrophobic films and could be used for food preservation. The water contact angle of CS/CMC/Y12 was similar to that of CS/CMC but was significantly lower than that of CS/CMC/Y11 ($p < 0.05$). This indicated that the hydrophobicity of CS/CMC was significantly enhanced after the addition of Y11.

3.5.4. Optical properties

The color of edible films is a crucial factor in determining their quality, as it has a direct impact on how consumers perceive and accept them (Galus & Lenart, 2013). To mimic the appearance of conventional packaging plastics, edible films should be nearly colorless. As shown in Table 1, the a-values (red to green) of CS/CMC/Y11 and CS/CMC/Y12 were lower ($p < 0.05$), and their b-values (yellow to blue) were higher ($p < 0.05$) than those of CS/CMC. This indicated that the addition of Y11 and Y12 shifted the color of the films towards the yellow-green spectrum. Moreover, the ΔE value of CS/CMC/Y12 was significantly reduced ($p < 0.05$). In summary, the color of CS/CMC/Y11 and CS/CMC/Y12 was more yellowish-green than that of CS/CMC, probably because both the Y11 and Y12 powder exhibited a yellow color in solution. It could be deduced from the optical image of the films (Fig. 2d) that the color of CS/CMC, CS/CMC/Y11, and CS/CMC/Y12 was yellowish. Overall, the color difference was mainly due to the addition of bacterial powder, but the color change due to the bacteria was quite limited. Moreover, no color change was observed in the films during the storage period, demonstrating the stability of the CS/CMC-based films.

The WI is also a key determinant of consumer acceptance and quality, and low WI values make products less favorable for consumers, especially fresh fruits like tomatoes (Das, Vishakha, Banerjee, Mondal, & Ganguli, 2020). The WI of the films (Table 1) varied from 60 to 65, and there was no statistically significant distinction between the WI of CS/CMC/Y11 and CS/CMC/Y12 and that of CS/CMC. Thus, consistent with the ΔE findings, the WI values also showed that the color changes in the edible films following bacterial addition were minimal.

Significantly, the opacity of CS/CMC/Y11 increased notably in comparison to CS/CMC, most likely because Y11 was included. The addition of the pale-yellow bacterial powder to the CS/CMC matrix enhanced the opacity of the resulting film. In summary, the findings showed that the addition of bacteria has little effect on the color of CS/CMC films. Although Y11 increases the opacity of the films, the opacity remains within 6–20 $A \cdot mm^{-1}$, and the difference in opacity is not extremely obvious. Therefore, the appearance characteristics of the edible films are in line with consumer preferences.

3.5.5. Mechanical properties

Food often experiences external pressure during processing, transportation, and storage. Thus, food packaging films must have sufficient mechanical strength and extensibility in order to maintain their integrity during the different stages of the food supply chain. From Table 1, it could deduced that there was no notable disparity in the TS values between CS/CMC/Y11 and CS/CMC/Y12 and those of CS/CMC TS. This indicated that the addition of Y11 and Y12 to the CS/CMC matrix does not change its tensile strength. However, the EBA of CS/CMC/Y12 was noticeably lower than that of CS/CMC ($p < 0.05$), but there was no significant disparity in the EBA value between CS/CMC/Y11 and CS/CMC. The results demonstrated that the inclusion of Y12 decreased the stretchability of the edible film. This could be attributed to the interference of bacterial cells with the interaction between macromolecules in the film solution during the film-forming process, leading to a decrease in the cohesion of the polymer network and thus lowering the film's ability to stretch.

3.6. FTIR spectroscopy

The composite films' intermolecular interactions were evaluated by FTIR spectroscopy. Fig. 3a illustrates the FTIR spectra of the edible films. The CS/CMC films exhibited a broad absorption band at 3583.74 cm^{-1}, which corresponds to the stretching vibration of the intermolecular O—H hydrogen bond. An absorption band was seen near 2922.16 cm^{-1}, indicating intermolecular C—H stretching vibrations. The peak observed at 1639.49 cm^{-1} can be attributed to the stretching vibrations of the C═O bond, while the peak at 1535.33 cm^{-1} corresponds to the asymmetric stretching vibration of the carboxylate group. The signal observed at 1438.39 cm^{-1} can be ascribed to the symmetric carboxylate group of CMC. The absence of any additional peaks in the composite film following the introduction of Y11 and Y12 indicates that the inclusion of bacteria does not modify the chemical composition of the CS/CMC matrix. López-Rubio, Sanchez, Wilkanowicz, Sanz, and Lagaron (2012) discovered that the presence of *Bifidobacterium* in a capsule made of whey protein concentrate and pullulan did not alter the chemical composition of the capsule material. Similarly, Nisar et al. (2022) created probiotic films by including four probiotic bacteria in citrus pectin films. It was observed that the presence of these bacteria did not cause any changes to the chemical composition of the matrix. These studies collectively demonstrate that including bacteria does not modify the chemical composition of the matrix in edible biofilms.

3.7. DSC analysis

The thermal characteristics of the edible films were analyzed using DSC. (Fig. 3b). All edible films showed two endothermic peaks and one exothermic peak. According to other reports (Kaczmarska et al., 2019), the first endothermic peak (100 °C–150 °C) is mainly caused by the dehydration of the material. The first endothermic peaks of CS/CMC, CS/CMC/Y11, and CS/CMC/Y12 were detected at 125.85 °C, 138.55 °C, and 127.35 °C, respectively. These findings indicated that CS/CMC/Y11 and CS/CMC/Y12 had a stronger water-binding capacity, and therefore,

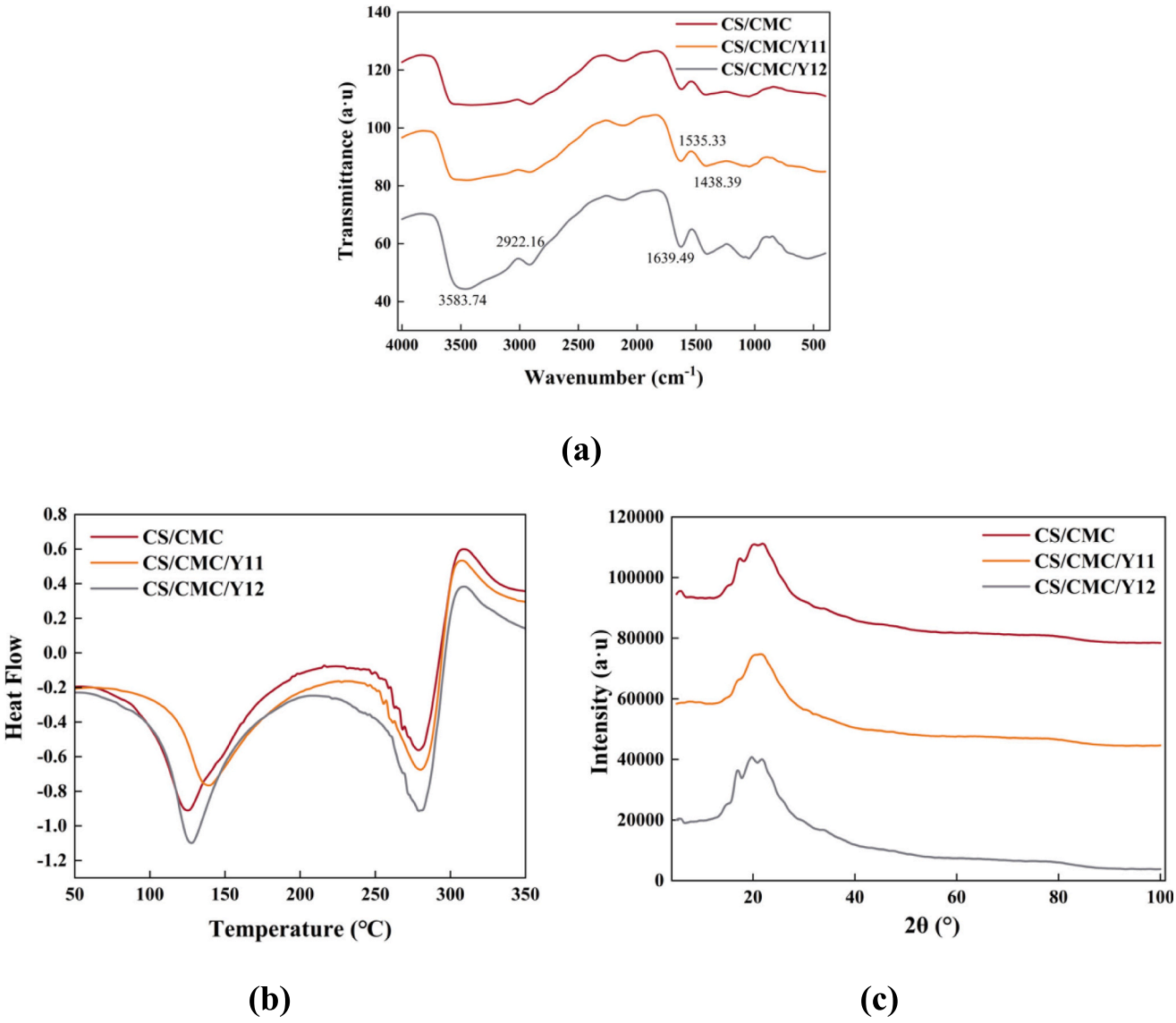

Fig. 3. Structural properties of films. (a) FTIR spectrum; (b) DSC analysis; (c) XRD spectrum.

their dehydration temperature was higher than that of CS/CMC. The second endothermic peak (250 °C–300 °C), and the primary cause is the disruption of the polymer chains in the films., i.e., the breakage of the bonds between the starch molecules in the polymer and the formation of volatile compounds. The second endothermic peak of all three films appeared at 279 °C, indicating that the polymeric structure of all these films was disrupted at 279 °C. Finally, an exothermic peak at 308 °C was detected in all three edible films. This peak represents thermal condensation between the hydroxyl groups on starch chains, resulting in the formation of ether segments. During this process, water molecules and other small molecules are released, and the adjacent hydroxyl groups in glucose rings are dehydrated, leading to the formation of C═C bonds and the destruction of glucose ring.

3.8. XRD analysis

Crystallinity is an important characteristic of composite films because it determines their properties and structure (Zhang et al., 2020). The crystalline region of a molecule contains a regular arrangement of atoms, while the amorphous region contains a random arrangement of atoms. Highly crystalline materials exhibit narrow and high peaks on XRD analysis, while those with low crystallinity show wide and low peaks. As shown in Fig. 3c, all the films exhibited a wide and low peak at $2\theta = 19.78°$ along with low crystallinity. These findings indicated that the samples had a semi-crystalline structure. According to other reports (Wang, Li, Copeland, Niu, & Wang, 2015), as a semi-crystalline material, natural starch shows varying XRD patterns and crystallinity characteristics, the wide peak at 19.78° might corresponding to the V-shaped diffraction peak of starch. Our results indicated that the incorporation of bacterial powders does not affect the crystal structure of the films.

3.9. Biodegradability

In soil, starch can be degraded via hydrolysis, microbial degradation, or both. Thus, soil embedding experiments are an effective way to study the biodegradability of starch films (Sanhawong et al., 2017). Microbial degradation is a complex process involving a variety of microorganisms, which convert the carbon in biopolymers into carbon dioxide and reintroduce them into the carbon cycle (Ferreira, Molina, & Pelissari, 2020). Soil parameters (temperature, pH, MC, and microbial density) can greatly influence the biodegradability of edible films (Nguyen, Do, Grillet, Thuc, & Thuc, 2016). Therefore, in this study, natural soil (temperature 25 °C, pH 6.0, MC around 45%) was selected to test the biodegradability of the prepared films. Fig. 4 shows the changes in the

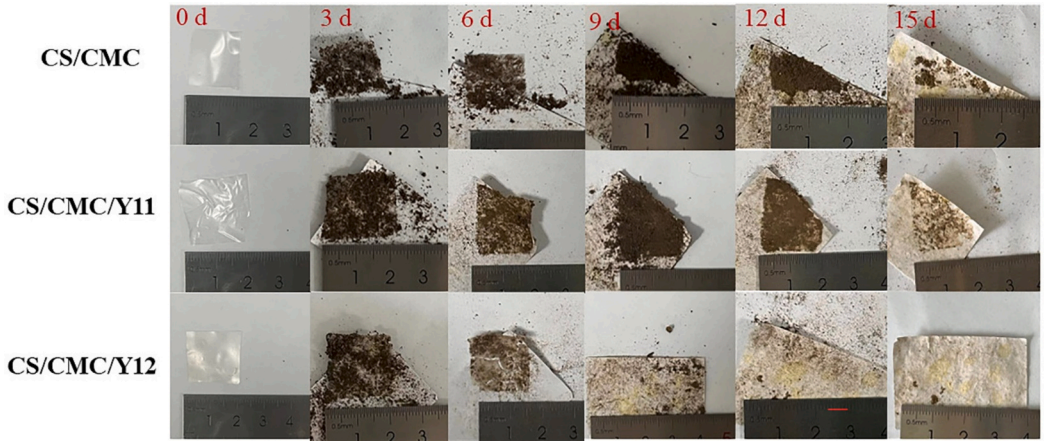

Fig. 4. Biodegradability of the film.

films within 15 days of soil burial. Notably, cracks appeared in the CS/CMC, CS/CMC/Y11, and CS/CMC/Y12 films on day 6. The CS/CMC/Y12 film could barely be detected by day 9, and CS/CMC and CS/CMC/Y11 were degraded into small pieces that were almost impossible to detect by day 15. The degradation of starch and CMC in the soil was complex and can be divided into two stages (Ferreira et al., 2020). The initial phase entails the uncomplicated hydrolysis and partial breakdown of starch and CMC. During the second phase, microbial enzymes break down the chemicals and generate polymer fragments on the films' surface, which can then be absorbed by soil bacteria. Our findings shown

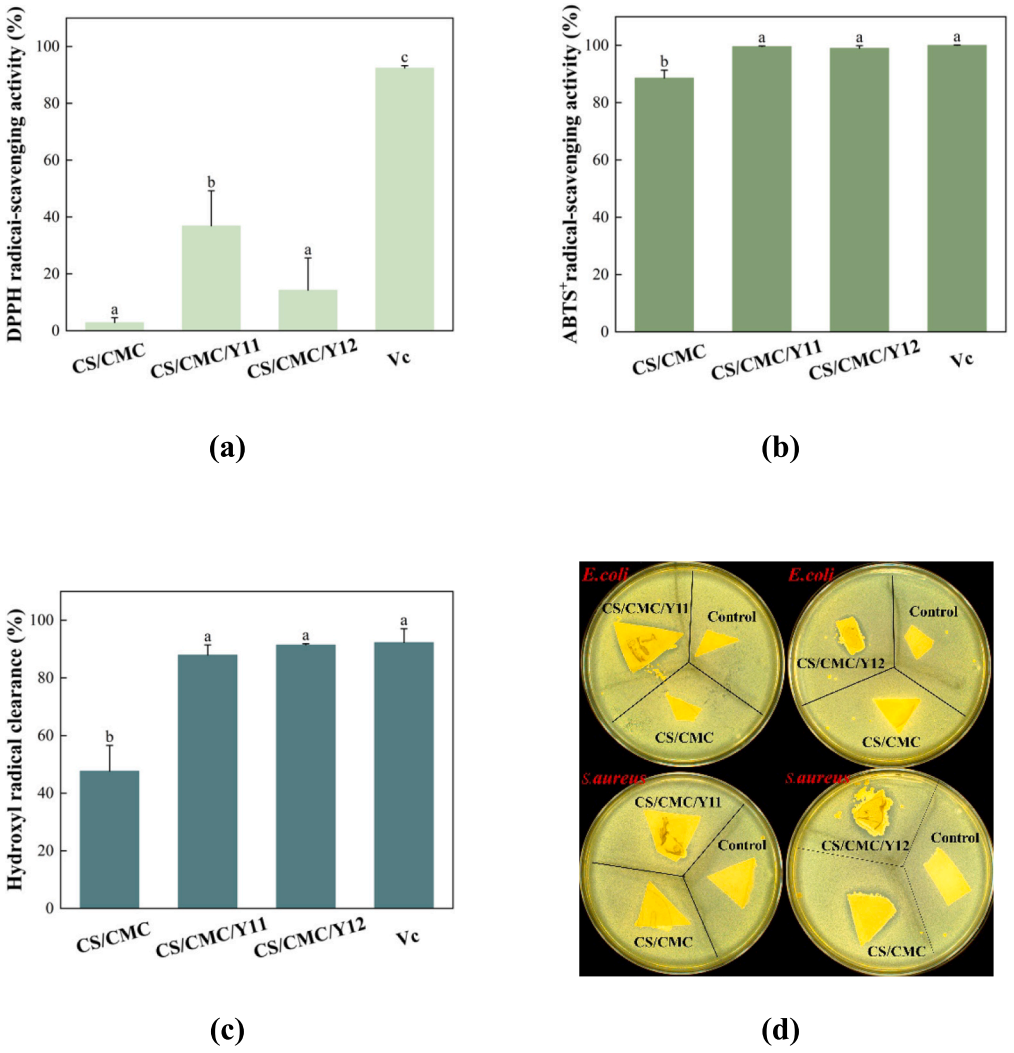

Fig. 5. The antioxidant and bacteriostatic capacity of films. (a) DPPH clearance; (b) $ABTS^{+}$ clearance; (c) Hydroxyl radical clearance; (d) Bacteriostat.
Notes: $^{a\text{-}c}$Different letters in the same row indicate significant differences under the same condition ($p < 0.05$).

that the films made from CS/CMC can undergo degradation by natural soil in a span of 15 days, regardless of the presence of Y11 and Y12. Therefore, these films can be employed in food packing to mitigate ecological contamination.

3.10. Antioxidant and antibacterial effects

Free radicals interact with cells and biomolecules in dietary items, leading to significant oxidative harm and thus diminishing the quality of food. As shown in Fig. 5a, the DPPH clearance rates of CS/CMC, CS/CMC/Y11, CS/CMC/Y12, and Vc were 3.00 ± 1.69%, 37.00 ± 12.33%,14.00 ± 11.31%, and 92.43 ± 0.82%, respectively. Compared with CS/CMC, the CS/CMC/Y11 film showed a 34% higher DPPH clearance rate, thus demonstrating a significant increase in DPPH scavenging ability ($p < 0.05$). Although the DPPH clearance rate of CS/CMC/Y12 was 11% higher than that of CS/CMC, this difference was not statistically significant. Together, the findings showed that Y11 could improve the DPPH clearing ability of CS/CMC, but Y12 failed to significantly enhance this parameter.

As shown in Fig. 5b, all the films exhibited the ability to clear $ABTS^+$. The $ABTS^+$ clearance rate of CS/CMC was 88.60 ± 1.10%, while that of CS/CMC/Y11, CS/CMC/Y12, and Vc was 99.59 ± 0.08%, 98.99 ± 0.35%, and 100.00 ± 0.10%, respectively. The $ABTS^+$ free-radical scavenging ability of CS/CMC/Y11 and CS/CMC/Y12 was 12.40% and 11.73% higher, respectively, than that of CS/CMC, representing a significant improvement ($p < 0.05$). Moreover, the $ABTS^+$ free-radical scavenging ability of CS/CMC/Y11 and CS/CMC/Y12 was comparable to that of Vc, indicating that both Y11 and Y12 could enhance the $ABTS^+$ clearing ability of CS/CMC.

Hydroxyl free radicals can easily cross edible films and react with biological macromolecules such as carbohydrates, proteins, and lipids, leading to cell death and food spoilage, moreover, hydroxyl radicals are the most toxic oxygen free radicals known at present (Purushothaman, Sheeja, & Janardanan, 2020). Therefore, hydroxyl radical scavenging is important for food preservation and the protection of biological systems. Fig. 5c shows the hydroxyl radical scavenging ability of CS/CMC, CS/CMC/Y11, and CS/CMC/Y12 (47.65 ± 8.90%, 87.95 ± 3.47%, and 91.42 ± 0.44%, respectively). The hydroxyl free radical scavenging ability of CS/CMC/Y11 and CS/CMC/Y12 was 84.57% and 91.86% higher ($p < 0.05$) than that of CS/CMC and comparable to that of Vc.

3.11. Bacteriostasis

Fig. 5d show the effect of the composite films on the growth of *E. coli* and *S. aureus*. It was indicated that adding Y11 and Y12 to CS/CMC could inhibit the growth of *E. coli*. The diameter of the inhibition zone against *E. coli* was comparable between CS/CMC/Y11 and CS/CMC/Y12, were around 0.29 mm, suggesting that both composite films exhibited similar antimicrobial activity against *E. coli*.

The inhibition zones of CS/CMC, CS/CMC/Y11, and CS/CMC/Y12 against *S. aureus* were 0.20 ± 0.05, 0.22 ± 0.04, and 0.33 ± 0.06 cm, respectively (Table 1). There was no significant difference in the diameter of the inhibition zone between CS/CMC and CS/CMC/Y11. However, the inhibition zone of CS/CMC/Y12 was significantly larger

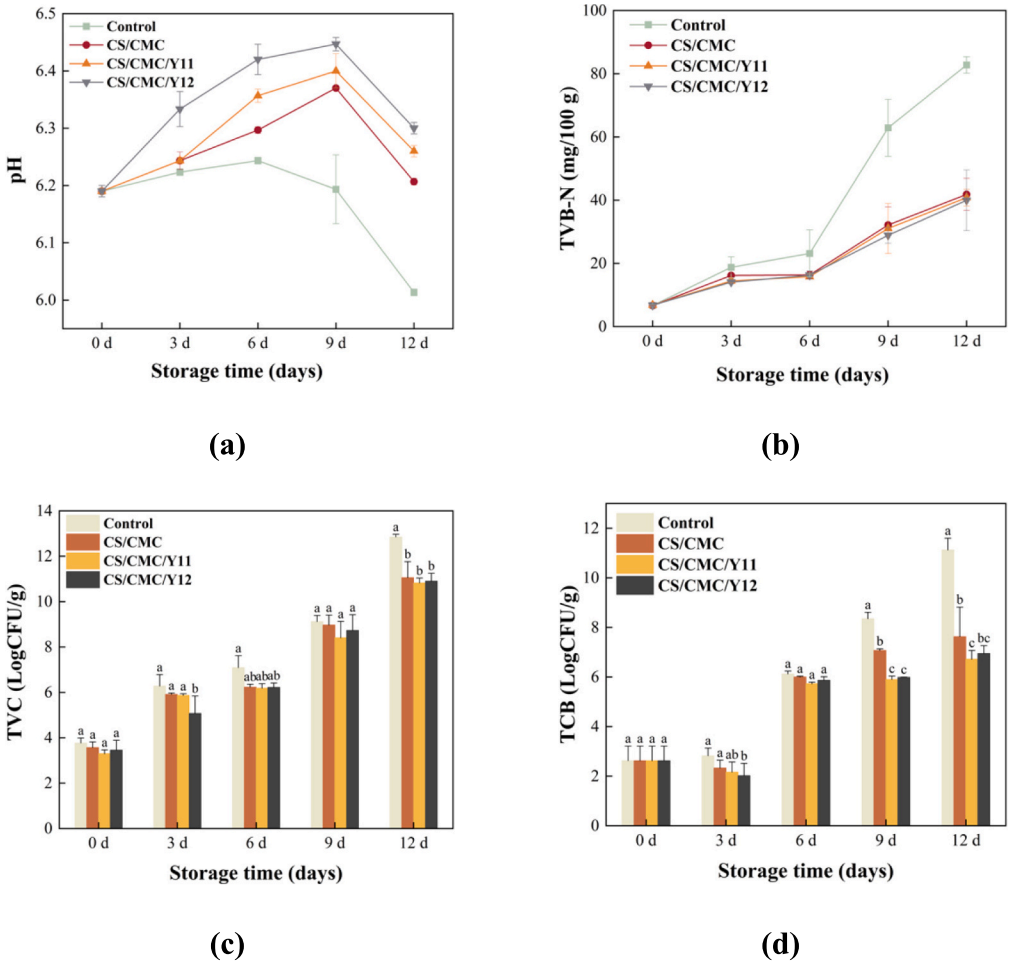

Fig. 6. The preservation effect of films on salmon. (a) pH; (b) TVB-N; (c) TVC; (d) TCB.
Notes: [a-c]Different letters in the same row indicate significant differences under the same condition ($p < 0.05$).

than that of CS/CMC against *S. aureus*, indicating that Y12 significantly enhances the antimicrobial activity of the composite film against *S. aureus*.

3.12. Salmon freshness

3.12.1. pH and TVB-N

The pH changes in salmon during storage are shown in Fig. 6a. As storage was prolonged, the pH of the salmon first increased and then decreased. The pH range of fresh fish is between 5.5 and 6.5. Even after 12 days of storage, the pH of all salmon samples remained within this range. However, the pH of the salmon samples coated with edible films was higher than that of uncoated ones; the highest pH was in the CS/CMC/Y12 group, and the lowest pH was in the CS/CMC group. The pH of the control group began to decline on day 6, while that of coated salmon samples began to decline on day 9, likely because the edible films inhibited the growth of the acid-producing microbe *S. aureus*. The decrease in the abundance of *S. aureus* could decrease the levels of acids, maintaining a higher pH in the salmon samples wrapped in edible films.

TVB-N serves as a chemical indicator for assessing the quality and duration of refrigerated seafood products (Arulkumar, Satheeshkumar, Paramasivam, Rameshthangam, & Miranda, 2020). The TVB-N concentration normally rises as a result of the proliferation of decomposing bacteria and the action of internal enzymes. Seafood with TVB-N levels over 35 mg/100 g are deemed unsuitable for ingestion (Chen et al., 2022). The TVB-N value of the fresh salmon samples was measured to be 6.68 ± 0.19 mg/100 g (Fig. 6a). Nevertheless, this value exhibited a progressive increase with the passage of time. However, the TVB-N levels were consistently lower in the salmon samples wrapped with edible films than in the uncoated salmon samples. The TVB-N was the highest among the CS/CMC group and the lowest among the CS/CMC/Y12 group. However, the difference between the two groups was not statistically significant. The TVB-N level in the control group samples surpassed the spoiling criterion on day 9. On day 12, the fish wrapped in the edible films only surpassed the spoiling threshold for TVB-N levels. Therefore, based on the TVB-N values, it can be concluded that the edible films have the ability to increase the shelf life of salmon by 3 days.

3.12.2. Microbiological analysis

The maximum allowable limit of TVC is 7.0 log CFU/g (Yu, Regenstein, & Xia, 2019). The changes in the TVC of salmon during storage are shown in Fig. 6c. The initial TVC of fresh salmon was 3.77 ± 0.22 log CFU/g, meeting the safety requirements. Within 12 days, the TVC gradually increased as storage was prolonged. On day 6, the control group had a TVC of >7.0 log CFU/g, with severe microbial spoilage. Meanwhile, no microbial spoilage was detected in the salmon covered with the edible film on day 6, and these samples only started to exhibit signs of microbial spoilage on day 9. These results showed that coating with the edible film could effectively extend the shelf life of salmon by about 3 days. The addition of Y11 and Y12 could enhance the antibacterial effect of the CS/CMC edible film, and CS/CMC/Y12 showed a significant antimicrobial effect on the 3rd day. Table 1 demonstrates that CS/CMC had an inhibitory effect on *S. aureus*, and CS/CMC/Y11 and CS/CMC/Y12 had an inhibitory effect on both *E. coli* and *S. aureus*. Therefore, the edible films exerted antibacterial effects, thus extending the shelf life of salmon. Notably, the addition of Y11 and Y12 enhanced this antibacterial effect.

Presently, the Joint Committee of the World Health Organization (WHO) and the Food and Agriculture Organization (FAO) Health and Nutrition Food Standards Program (CAC) have set the TCB limit at 4.00 log CFU/g. Fig. 6d illustrates the alterations in TCB in salmon over the process of storage. The initial TCB in fresh salmon samples was 2.62 ± 0.59 log CFU/g, which complies with the safety standards. Nevertheless, the TCB exhibited a progressive increase in correlation with the increase in storage time. On the 6th day, the TCB value of each group was above 3.70 log CFU/g, suggesting that the salmon had spoiled. The TCB in the CS/CMC/Y11 and CS/CMCY12 groups on day 9 did not show a statistically significant increase compared to day 6. In addition, the TCB of the CS/CMC/Y11 and CS/CMC/Y12 groups was notably lower than that of the control group and CS/CMC group on day 9 and day 12. This suggests that the CS/CMC/Y11 and CS/CMC/Y12 films effectively suppressed the growth of *E. coli*.

3.12.3. The color and texture profile analysis

During storage, the color and texture profile alter due to protein denaturation and microbial degradation. Fig. 7 (a-e) shows the color change of the salmon flesh during 4 °C storage. With the extension of the storage time, the color of the salmon gradually becomes brown, and the values of brightness (L), red (a), yellow (b), and total color difference (△E) show a downward trend, which mainly due to protein oxidation and pigment accumulation of microbial spoilage (Wang, Zhang, Jin, & Li, 2018). However, the L value of the CS/CMC/Y12 film on day 9 and the a and △E values of the CS/CMC/Y11 film on day 9 and day 6 were significantly higher than the control group, which indicated that these films would retard the protein oxidation and bacteria growth, which was in accordance with the TVB-N and microbial analysis results. Our results indicated the edible film with the *Bacillus* strains would be beneficial to maintaining the color of the salmon flesh.

Fig. 7 (f-i) shows the hardness, elasticity, cohesiveness, and chewability of the salmon during 12 days of storage. The texture indexes decreased mainly due to the loss of water and myogenic protein (Wang et al., 2024). On day 12, the cohesiveness of the CS/CMC/Y11 and CS/CMC/Y12 films groups were significantly higher than the control group, which indicated that the edible film with the addition of *Bacillus* strains would help to maintain the cohesiveness of the salmon flesh. For hardness and chewiness, the CS/CMC/Y12 film had equal performance as the CS/CMC film on salmon flesh; the values were higher than CS/CMC/Y11 film and the unpackaged group, which might be due to the addition of different strains.

4. Conclusion

In this study, Y11 and Y12 were successfully incorporated into a CS, CMC, and glycerol-based edible film. Notably, the addition of Y11 and Y12 did not change the physical properties of the CS/CMC matrix; however, it improved the edible film's antioxidant and antibacterial abilities. When used to preserve salmon flesh, the chemical, microbial, and texture profile analysis showed that the edible films could extend the shelf life of salmon by about 3 days.

In the future study, we will pay more attention to another edible film matrix other than CS and CMC to improve the performance of the edible film embedded with *Bacillus*. Moreover, the metabolic activities of the *Bacillus* strains in the film matrix, for instance, the release of the bacteriocin or other metabolic, could also be investigated, and the function of the EPS produced by the *Bacillus* in the edible film would need to be further explored.

CRediT authorship contribution statement

Xiqian Tan: Writing – review & editing, Writing – original draft, Methodology, Formal analysis, Conceptualization. **Anqi Sun:** Writing – original draft, Methodology. **Fangchao Cui:** Formal analysis, Data curation. **Qiuying Li:** Methodology, Formal analysis. **Dangfeng Wang:** Investigation. **Xuepeng Li:** Writing – review & editing, Supervision. **Jianrong Li:** Writing – review & editing, Supervision, Funding acquisition.

Declaration of competing interest

The authors declare that they have no known competing financial interests or personal relationships that could have influenced the work reported in this paper.

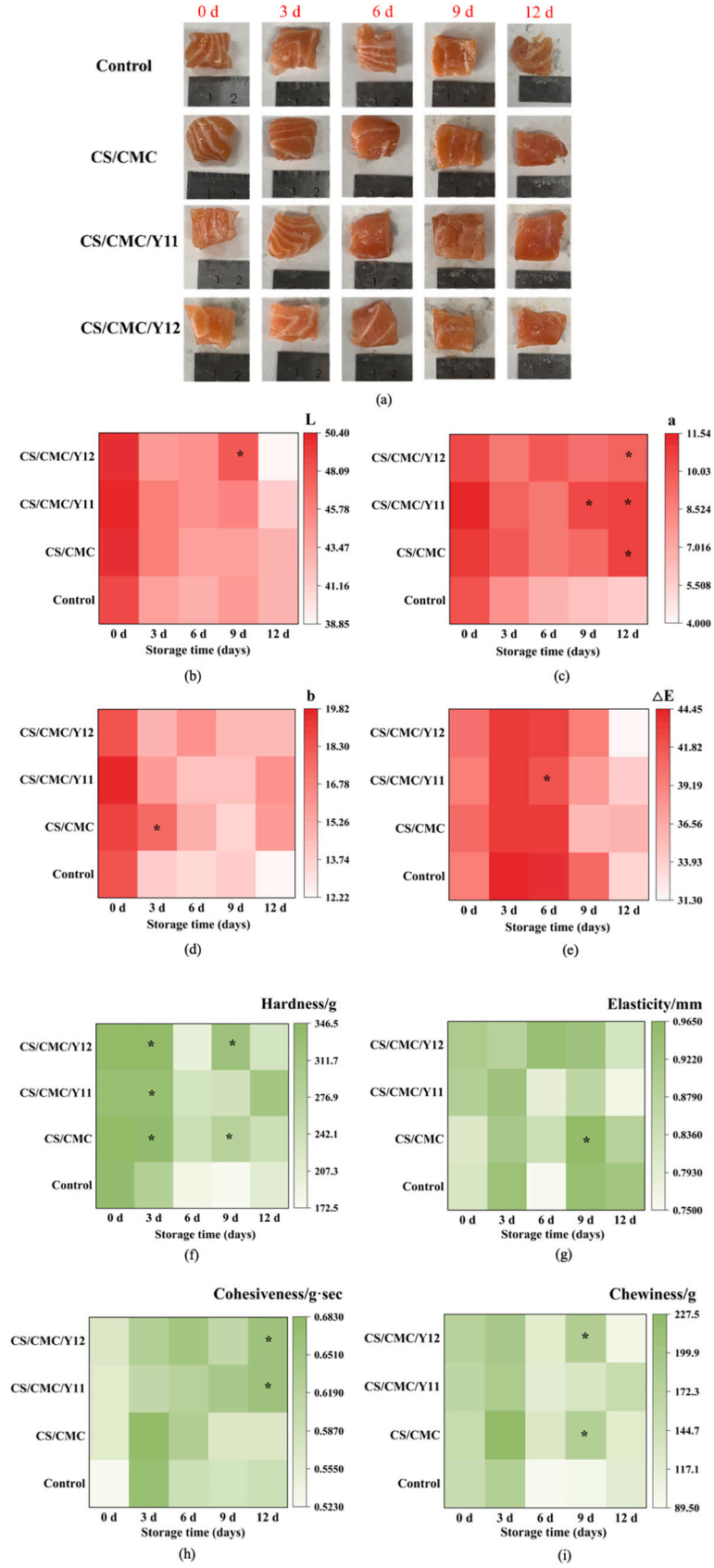

Fig. 7. The color and texture changes of the salmon pieces. (a) Optical image of the salmon pieces; (b) L value; (c) a value; (d) b value (e) △E value; (f) Hardness; (g) Elasticity; (h) Cohesiveness; (i) Chewability;
Note: * indicated the significant differences under the same condition ($p < 0.05$).

Data availability

No data was used for the research described in the article.

Acknowledgments

This work was supported by the National Key Research and Development Program of China (2019YFD0901702).

We appreciate those who help directly and indirectly with this work.

References

Abdollahzadeh, E., Nematollahi, A., & Hosseini, H. (2021). Composition of antimicrobial edible films and methods for assessing their antimicrobial activity: A review. *Trends in Food Science & Technology, 110*, 291–303. https://doi.org/10.1016/j.tifs.2021.01.084

Al-Harrasi, A., Bhatia, S., Al-Azri, M. S., Ullah, S., Najmi, A., Albratty, M., … Aldawsari, M. F. (2022). Effect of drying temperature on physical, chemical, and antioxidant properties of ginger oil loaded gelatin-sodium alginate edible films. *Membranes, 12*, 862. https://doi.org/10.3390/membranes12090862

Arulkumar, A., Satheeshkumar, K., Paramasivam, S., Rameshthangam, P., & Miranda, J. M. (2020). Chemical biopreservative effects of red seaweed on the shelf life of black tiger shrimp (*Penaeus monodon*). *Foods, 9*, 634. https://doi.org/10.3390/foods9050634

Bangyekan, C., Aht-Ong, D., & Srikulkit, K. (2006). Preparation and properties evaluation of chitosan-coated cassava starch films. *Carbohydrate Polymers, 63*, 61–71. https://doi.org/10.1016/j.carbpol.2005.07.032

Ceylan, H. G., & Atasoy, A. F. (2023). Synbiotic edible films enriched with probiotics and prebiotics: A novel approach for improving the quality and shelf life of sliced cheese. *Packaging Technology and Science, 36*, 1005–1019. https://doi.org/10.1002/pts.2771

Chen, J., Yang, R., Wang, Y., Koseki, S., Fu, L., & Wang, Y. (2022). Inhibitory effect of d-tryptophan on the spoilage potential of *Shewanella baltica* and *Pseudomonas fluorescens* and its potential application in salmon fillet preservation. *Food Microbiology, 108*, Article 104104. https://doi.org/10.1016/j.fm.2022.104104

Chowdhury, S. P., Hartmann, A., Gao, X., & Borriss, R. (2015). Biocontrol mechanism by root-associated *Bacillus amyloliquefaciens* FZB42 – A review. *Frontiers in Microbiology, 6*, 780. https://doi.org/10.3389/fmicb.2015.00780

Das, S., Vishakha, K., Banerjee, S., Mondal, S., & Ganguli, A. (2020). Sodium alginate-based edible coating containing nanoemulsion of Citrus sinensis essential oil eradicates planktonic and sessile cells of food-borne pathogens and increased quality attributes of tomatoes. *International Journal of Biological Macromolecules, 162*, 1770–1779. https://doi.org/10.1016/j.ijbiomac.2020.08.086

Davachi, S. M., Pottackal, N., Torabi, H., & Abbaspourrad, A. (2021). Development and characterization of probiotic mucilage based edible films for the preservation of fruits and vegetables. *Scientific Reports, 11*, Article 16608. https://doi.org/10.1038/s41598-021-95994-5

Dehghani, S., Hosseini, S. V., & Regenstein, J. M. (2018). Edible films and coatings in seafood preservation: A review. *Food Chemistry, 240*, 505–513. https://doi.org/10.1016/j.foodchem.2017.07.034

Espitia, P. J. P., Batista, R. A., Azeredo, H. M. C., & Otoni, C. G. (2016). Probiotics and their potential applications in active edible films and coatings. *Food Research International, 90*, 42–52. https://doi.org/10.1016/j.foodres.2016.10.026

Ferreira, D. C. M., Molina, G., & Pelissari, F. M. (2020). Biodegradable trays based on cassava starch blended with agroindustrial residues. *Composites Part B: Engineering, 183*, Article 107682. https://doi.org/10.1016/j.compositesb.2019.107682

Fu, N., & Chen, X. D. (2011). Towards a maximal cell survival in convective thermal drying processes. *Food Research International, 44*, 1127–1149. https://doi.org/10.1016/j.foodres.2011.03.053

Galus, S., & Lenart, A. (2013). Development and characterization of composite edible films based on sodium alginate and pectin. *Journal of Food Engineering, 115*, 459–465. https://doi.org/10.1016/j.jfoodeng.2012.03.006

Ghanbarzadeh, B., Almasi, H., & Entezami, A. A. (2010). Physical properties of edible modified starch/carboxymethyl cellulose films. *Innovative Food Science & Emerging Technologies, 11*, 697–702. https://doi.org/10.1016/j.ifset.2010.06.001

Gholam-Zhiyan, A., Amiri, S., Rezazadeh-Bari, M., & Pirsa, S. (2021). Stability of *Bacillus coagulans* IBRC-M 10807 and *Lactobacillus plantarum* PTCC 1058 in Milk proteins concentrate (MPC)-based edible film. *Journal of Packaging Technology and Research, 5*, 11–22. https://doi.org/10.1007/s41783-021-00106-3

Gürdal, A. A., & Çetinkaya, T. (2023). Advancements in edible films for aquatic product preservation and packaging. *Reviews in Aquaculture*. https://doi.org/10.1111/raq.12880

Jaderi, Z., Yazdi, F. T., Mortazavi, S. A., & Koocheki, A. (2023). Effects of glycerol and sorbitol on a novel biodegradable edible film based on *Malva sylvestris* flower gum. *Food Science & Nutrition, 11*, 991–1000. https://doi.org/10.1002/fsn3.3134

Kaczmarska, K., Żymankowska-Kumon, S., Byczyński, Ł., Grabowska, B., Bobrowski, A., & Cukrowicz, S. (2019). Thermoanalytical studies (TG–DTG–DSC, Py–GC/MS) of sodium carboxymethyl starch with different degrees of substitution. *Journal of Thermal Analysis and Calorimetry, 138*, 4417–4425. https://doi.org/10.1007/s10973-019-08892-4

Kanmani, P., & Lim, S. T. (2013). Development and characterization of novel probiotic-residing pullulan/starch edible films. *Food Chemistry, 141*, 1041–1049. https://doi.org/10.1016/j.foodchem.2013.03.103

Lacey, A. M. L.d., López-Caballero, M. E., Gómez-Estaca, J., Gómez-Guillén, M. C., & Montero, P. (2012). Functionality of *lactobacillus acidophilus* and *Bifidobacterium bifidum* incorporated to edible coatings and films. *Innovative Food Science & Emerging Technologies, 16*, 277–282. https://doi.org/10.1016/j.ifset.2012.07.001

Lan, W., Zhang, R., Ji, T., Sameen, D. E., Ahmed, S., Qin, W., … Liu, Y. (2021). Improving nisin production by encapsulated *Lactococcus lactis* with starch/carboxymethyl cellulose edible films. *Carbohydrate Polymers, 251*, Article 117062. https://doi.org/10.1016/j.carbpol.2020.117062

Li, T., Zhang, X., Mei, J., Cui, F., Wang, D., & Li, J. (2022). Preparation of linalool/polycaprolactone coaxial electrospinning film and application in preserving salmon slices. *Frontiers in Microbiology, 13*, Article 860123. https://doi.org/10.3389/fmicb.2022.860123

Lin, D., Zheng, Y., Wang, X., Huang, Y., Ni, L., Chen, X., Wu, Z., Huang, C., Yi, Q., Li, J., Qin, W., Zhang, Q., Chen, H., & Wu, D. (2020). Study on physicochemical properties, antioxidant and antimicrobial activity of okara soluble dietary fiber/sodium carboxymethyl cellulose/thyme essential oil active edible composite films incorporated with pectin. *International Journal of Biological Macromolecules, 165*, 1241–1249. https://doi.org/10.1016/j.ijbiomac.2020.10.005

Lin, L., Peng, S., Chen, X., Li, C., & Cui, H. (2023). Silica nanoparticles loaded with caffeic acid to optimize the performance of cassava starch/sodium carboxymethyl cellulose film for meat packaging. *International Journal of Biological Macromolecules, 241*, Article 124591. https://doi.org/10.1016/j.ijbiomac.2023.124591

López-Rubio, A., Sanchez, E., Wilkanowicz, S., Sanz, Y., & Lagaron, J. M. (2012). Electrospinning as a useful technique for the encapsulation of living *bifidobacteria* in food hydrocolloids. *Food Hydrocolloids, 28*, 159–167. https://doi.org/10.1016/j.foodhyd.2011.12.008

Ma, D., Jiang, Y., Ahmed, S., Qin, W., & Liu, Y. (2020). Antilisterial and physical properties of polysaccharide-collagen films embedded with cell-free supernatant of *Lactococcus lactis*. *International Journal of Biological Macromolecules, 145*, 1031–1038. https://doi.org/10.1016/j.ijbiomac.2019.09.195

Majeed, M., Majeed, S., Nagabhushanam, K., Natarajan, S., Sivakumar, A., & Ali, F. (2016). Evaluation of the stability of *Bacillus coagulans* MTCC 5856 during processing and storage of functional foods. *International Journal of Food Science & Technology, 51*, 894–901. https://doi.org/10.1111/ijfs.13044

Mantovan, J., Bersaneti, G. T., Faria-Tischer, P. C. S., Celligoi, M. A. P. C., & Mali, S. (2018). Use of microbial Levan in edible films based on cassava starch. *Food Packaging and Shelf Life, 18*, 31–36. https://doi.org/10.1016/j.fpsl.2018.08.003

Nazir, S., & Wani, I. A. (2022). Development and characterization of an antimicrobial edible film from basil seed (*Ocimum basilicum* L.) mucilage and sodium alginate. *Biocatalysis and Agricultural Biotechnology, 44*, Article 102450. https://doi.org/10.1016/j.bcab.2022.102450

Nguyen, D. M., Do, T. V. V., Grillet, A.-C., Thuc, H. H., & Thuc, C. N. H. (2016). Biodegradability of polymer film based on low density polyethylene and cassava starch. *International Biodeterioration & Biodegradation, 115*, 257–265. https://doi.org/10.1016/j.ibiod.2016.09.004

Nisar, T., Alim, A., Iqbal, T., Iqbal, M., Tehseen, S., Zi-Chao, W., & Guo, Y. (2022). Functionality of different probiotic strains embedded in citrus pectin based edible films. *International Journal of Food Science & Technology, 57*, 1005–1015. https://doi.org/10.1111/ijfs.15460

Pereira, J. O., Soares, J., Sousa, S., Madureira, A. R., Gomes, A., & Pintado, M. (2016). Edible films as carrier for lactic acid bacteria. *LWT - Food Science and Technology, 73*, 543–550. https://doi.org/10.1016/j.lwt.2016.06.060

Purushothaman, A., Sheeja, A. A., & Janardanan, D. (2020). Hydroxyl radical scavenging activity of melatonin and its related indolamines. *Free Radical Research, 54*, 373–383. https://doi.org/10.1080/10715762.2020.1774575

Razmjoo, F., Sadeghi, E., Rouhi, M., Mohammadi, R., Noroozi, R., & Safajoo, S. (2021). Polyvinyl alcohol–Zedo gum edible film: Physical, mechanical and thermal properties. *Journal of Applied Polymer Science, 138*, 49875. https://doi.org/10.1002/app.49875

Saleena, L. A. K., Kumaran, D., How, Y., & Pui, L. (2023). Probiotic-edible film in active packaging with antimicrobial effect and storage viability: A review. *International Journal of Food Science and Technology*. https://doi.org/10.1111/ijfs.16806

Sanhawong, W., Banhalee, P., Boonsang, S., & Kaewpirom, S. (2017). Effect of concentrated natural rubber latex on the properties and degradation behavior of cotton-fiber-reinforced cassava starch biofoam. *Industrial Crops and Products, 108*, 756–766. https://doi.org/10.1016/j.indcrop.2017.07.046

Socaciu, M.-I., Fogarasi, M., Semeniuc, C. A., Socaci, S. A., Rotar, M. A., Mureşan, V., … Vodnar, D. C. (2020). Formulation and characterization of antimicrobial edible films based on whey protein isolate and tarragon essential oil. *Polymers, 12*, 1748. https://doi.org/10.3390/polym12081748

Tan, X., Wang, D., Cheng, X., Li, X., & Li, J. (2023). Screening and probiotic characteristics of shrimp paste originated *Bacillus* spp. *Journal of Chinese Institute of Food Science and Technology, 23*, 51–61. https://doi.org/10.16429/j.1009-7848.2023.12.006

Wang, F., Zhang, H., Jin, W., & Li, L. (2018). Effects of tartary buckwheat polysaccharide combined with nisin edible coating on the storage quality of tilapia (*Oreochromis niloticus*) fillets. *Journal of the Science of Food and Agriculture, 98*(8), 2880–2888. https://doi.org/10.1002/jsfa.8781

Wang, S., Li, C., Copeland, L., Niu, Q., & Wang, S. (2015). Starch retrogradation: A comprehensive review. *Comprehensive Reviews in Food Science and Food Safety, 14*, 568–585. https://doi.org/10.1111/1541-4337.12143

Wang, Z., Qiao, F., Zhang, W., Parisi, G., Du, Z., & Zhang, M. (2024). The flesh texture of teleost fish: Characteristics and interventional strategies. *Reviews in Aquaculture, 16*(1), 508–535. https://doi.org/10.1111/raq.12849

Xie, Q., Liu, G., Zhang, Y., Yu, J., Wang, Y., & Ma, X. (2023). Active edible films with plant extracts: A updated review of their types, preparations, reinforcing properties,

and applications in muscle foods packaging and preservation. *Critical Reviews in Food Science and Nutrition, 63*, 11425–11447. https://doi.org/10.1080/10408398.2022.2092058

Ye, S., Zhu, Z., Wen, Y., Su, C., Jiang, L., He, S., & Shao, W. (2019). Facile and green preparation of pectin/cellulose composite films with enhanced antibacterial and antioxidant behaviors. *Polymers, 11*, 57. https://doi.org/10.3390/polym11010057

Yu, D., Regenstein, J. M., & Xia, W. (2019). Bio-based edible coatings for the preservation of fishery products: A review. *Critical Reviews in Food Science and Nutrition, 59*, 2481–2493. https://doi.org/10.1080/10408398.2018.1457623

Zhang, Y., Zhou, L., Zhang, C., Show, P. L., Du, A., Fu, J., & Ashokkumar, V. (2020). Preparation and characterization of curdlan/polyvinyl alcohol/thyme essential oil blending film and its application to chilled meat preservation. *Carbohydrate Polymers, 247*, Article 116670. https://doi.org/10.1016/j.carbpol.2020.116670